Hindawi
Wireless Communications and Mobile Computing
Volume 2020, Article ID 8839088, 13 pages
https://doi.org/10.1155/2020/8839088

*Research Article*

# Energy Efficiency Augmentation in Massive MIMO Systems through Linear Precoding Schemes and Power Consumption Modeling

**Rao Muhammad Asif,[1] Jehangir Arshad,[2] Mustafa Shakir,[1] Sohail M. Noman,[3] and Ateeq Ur Rehman[4,5]**

[1]*Department of Electrical Engineering, The Superior College Lahore, Lahore, Pakistan*
[2]*Electrical and Computer Engineering Department, COMSATS University Islamabad, Lahore Campus, Lahore 54000, Pakistan*
[3]*Department of Cell Biology and Genetics, Shantou University Medical College, Shantou, Guangdong 515041, China*
[4]*College of Internet of Things Engineering, Hohai University, Changzhou 213022, China*
[5]*Department of Electrical Engineering, Government College University, Lahore 54000, Pakistan*

Correspondence should be addressed to Jehangir Arshad; jehangirarshad@cuilahore.edu.pk

Received 28 April 2020; Revised 17 August 2020; Accepted 27 August 2020; Published 17 September 2020

Academic Editor: Enrico M. Vitucci



Massive multiple-input multiple-output or massive MIMO system has great potential for 5$^{th}$ generation (5G) wireless communication systems as it is capable of providing game-changing enhancements in area throughput and energy efficiency (EE). This work proposes a realistic and practically implementable EE model for massive MIMO systems while a general and canonical system model is used for single-cell scenario. Linear processing schemes are used for detection and precoding, i.e., minimum mean squared error (MMSE), zero-forcing (ZF), and maximum ratio transmission (MRT/MRC). Moreover, a power dissipation model is proposed that considers overall power consumption in uplink and downlink communications. The proposed model includes the total power consumed by power amplifier and circuit components at the base station (BS) and single antenna user equipment (UE). An optimal number of BS antennas to serve total UEs and the overall transmitted power are also computed. The simulation results confirm considerable improvements in the gain of area throughput and EE, and it also shows that the optimum area throughput and EE can be realized wherein a larger number of antenna arrays at BS are installed for serving a greater number of UEs.

## 1. Introduction and Related Studies

In existing 3G and 4G standards, BS allows only up to 8 antenna ports. However, the BS antennas for 5G standard are increased to support data transmission rate up to several GBs/seconds. The enhancements are forecasted to be achieved through the techniques, i.e., network densification (extra BS nodes), amplified bandwidth (mm-wave spectrum) or by using massive MIMO systems. Massive MIMO systems are multicarrier systems with "L" cells that use time division duplex operation protocol. In this system, to realize channel hardening, BS is prepared with $M$ number of antennas where each BS communicate with $N$ number of UEs instantaneously. Realizing unbounded EE is impossible because the system model does not consider the power expended by analog circuits (for radio frequency (RF) and baseband processing) and signal processing that raises linearly with $M$ and $N$. Hence, it can be taken as constant only in massive MIMO setups where values of $M$ and $N$ are comparatively small, while its changeability can be observed in massive MIMO systems in which, $(M, N \gg 1)$. The definition of massive MIMO in [1] also supposed the ration of $M$ and $N \gg 1$, while in [2, 3], the ratio has been taken as a small constant value. All BS process its signals independently by using linear transmit precoding and received combining. We have considered a canonical massive MIMO system model that

is implementable in real-time testbeds. Massive MIMO system shows many advantages over MIMO systems low power consumption because of enlarged antenna aperture and improved network capacity [2]. So far, efficient modeling of power consumption is a protuberant apprehension of these systems. Especially, in mobile UEs, the battery technology is not improving as per the massively rising demand for multimedia communication [3]. Analyzing a massive MIMO network for realistic modeling of total power consumption during uplink and downlink communications as it plays a vital role to achieve optimal area throughput, and maximum EE is a prominent aim of this work. Area throughput and EE can be defined as Definitions 1 and 2, respectively.

*Definition 1.* Total bits successfully transmitted per kilometer in one second is called area throughput measured as bits-per-Joule [4].

$$\text{Area throughput} = \frac{(\text{Available data rate})}{(\text{Area of cell})} = \frac{(\text{bits/sec})}{\text{km}^2}. \quad (1)$$

*Definition 2.* Total bits successfully transmitted by consuming a Joule of energy is called EE measured as bits-per-Joule [4]. In massive MIMO systems, EE is dependent on many factors, i.e., spectral efficiency, network architecture, power consumption by the entire system, and transmission protocol [4–9]. Existing literature provides mathematical modeling of mentioned parameters to enhance area throughput and EE. In [10], authors have provided an exhaustive power consumption modeling for EE optimization. Moreover, the circuit power utilization impact on transmitting antenna is deliberated by authors in [11–17]. Specifically, [13] emphasizes on uplink communication and power consumption of the massive MIMO network in uplink communication. Authors determined the optimized EE while the antennas of UEs are turned off. In [14–16], authors examine the downlink communication of a system and concluded EE as a concave function of total antennas at BS. In [17–21], authors provide the optimum value of $M$ to attain the maximum EE of a multicell scenario for a specified number of UEs. Authors in [22–26] modeled the EE by efficient power allocation for uplink and downlink by using MMSE processing scheme. Realization of infinite throughput and EE is perceptibly unrealistic because the power required for signal processing and analog circuits increases with increasing values of $M$ [9–13]. However, existing literature claims that it is possible to attain infinite EE because most of the modeling has been done by neglecting the impact of an increasing number of UEs.

The primary concentration of this paper is to mathematically model the impact of $M$, $N$, and the total power utilization on EE of a massive MIMO architecture by using linear processing schemes, i.e., MMSE, MRT/MRC, and ZF. We have also illustrated how energy hoarding help to improve the area throughput and EE at the network level. The second objective is to deliver an accurate power dissipation model that encompasses the power consumed by the entire system during uplink and downlink communication. Additionally, the linear precoding and received combining schemas are used including MMSE, ZF (perfect/imperfect CSI), and MRT/MRC at BS and UEs. The resulting expression (38) gives understandings of the impact of atmospheric effects during propagation, structural parameters, and the hardware apparatuses cast off to originate the power utilization modeling. Prescribed objectives are well achieved and outcomes are summarized as follows.

(i) MMSE and ZF schemes carry the max EE gain; however, ZF is better as compared with min square root error and MRT because of less complexity and better interference mitigation practice

(ii) Total circuit power and transmit power increase by increasing BS antennas

(iii) BS has hundreds of antennas that is an utmost efficient way to serve UE with optimal EE and area throughput

(iv) The ratio of reducing cell size is also applied as provided in [26] expression (40). According to the expression cell, radius and user density values are set accordingly. Reducing cell radius decreases the network capacity of the system; however, it increases the EE.

Listed results are appropriate to authenticate the massive MIMO architecture that it is an accurate method to attain the maximum EE in $5^{\text{th}}$ generation cellular networks. The remaining sections of this paper are structured as follows. Uplink and Downlink Massive MIMO System Model illustrates the canonical massive MIMO system model for both uplink and downlink communication. Additionally, it also describes the user distribution and linear precoding schemes. Later on, Methodology and Calculations is the main section as it includes all significant mathematical modeling and computations of data rate and power utilization model. Optimization of $M$, $N$, power, area throughput, and EE is articulated in the same Methodology and Calculations. Moreover, Results and Discussion stretches results to validate the theoretic analysis and draws the contrasts of the proposed model by using prescribed linear processing schemes with existing works. Finally, key insinuation conclusions are drawn in Conclusions. Table 1 shows the symbolic presentations used in this paper.

## 2. Uplink and Downlink Massive MIMO System Model

The following segment represents the specifications of massive MIMO network covering the distribution of users, linear processing scheme, and channel model. A single-cell case is cogitated in which $M$ numbers of transmit antennas are employed to attend $N$ single antenna UEs. Furthermore, the flat-fading channel is considered for transmission which is delimited by coherence time-frequency blocks as characterized by $S_{\text{CB}}$. Time division duplex is used for an operation

Table 1: Symbolic Representations.

| Symbols | Description |
|---|---|
| $\mathbb{E}(.)$ | Expectation |
| $\lvert . \rvert$ and $\lVert . \rVert$ | Absolute values and Euclidean norm |
| $\boldsymbol{I}_K$ | $K \times K$ identity matrix |
| $\mathbf{0}_K$ and $\mathbf{1}_K$ | $K$-dimensional null and unit column vectors |
| $\mathscr{CN}(.,.)$ | Multivariant circularly symmetric complex Gaussian distribution |
| $B$ | Bandwidth |
| $T_{\text{coh}}$ and $B_{\text{coh}}$ | Coherence time and coherence bandwidth |
| $S_{\text{CB}}$ | Coherence time-frequency ($S_{\text{CB}} = T_{\text{coh}} * B_{\text{coh}}$) |
| $\gamma^{(\text{UL})}$ and $\gamma^{(\text{DL})}$ | Constant transmission ratio symbols (uplink and downlink) |
| $S_{\text{CB}} * \gamma^{(\text{UL})}$ and $S_{\text{CB}} * \gamma^{(\text{DL})}$ | Uplink transmission and downlink transmission |

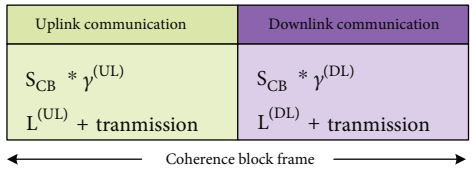


Figure 1: Coherence block frame: uplink/downlink transmissions.

mode because the BS and UEs are copiously synchronized to each other. Figure 1 provides a demonstration of TDD coherence block frame for bidirectional transmissions.

The uplink pilots are used at the BS to estimate the channels of UEs, whereas the downlink pilots are used at UE for estimating the interference and at the channel by using linear precoding schemes [11]. Prearranged channel massive MIMO model is considered because it enables the allocation of antenna correlation and path loss component. Additionally, it permits considerable antenna correlation of antenna either due to less antenna spacing or the absence of scattering f4or large antenna arrays [21, 22]. Various types of antenna configuration are proposed for massive MIMO systems in the literature including cylinder configuration, linear configuration, and rectangular configuration [23–25]. We have considered the cylinder configuration. Moreover, MMSE, MRT, and ZF processing and detection techniques are operational in these networks that help to reduce power consumption significantly; however, the overall circuit power dissipation upsurges progressively by growing $M$ [19]. Received vector at $l^{\text{th}}$ BS is denoted with $Y_l$, $Y_l \in \mathbb{C}^{\text{M}}$ given as

$$Y_l = \sum_{l=1}^{N} G\sqrt{\rho_l^{Tx}} x_l + n_l. \tag{2}$$

The $M \times N$ matrix between BS and UE is specified by $G$ in equation (2). The channel coefficients among $l^{\text{th}}$ UE and $i^{\text{th}}$ BS antenna are identified as ($g_{il} \triangleq G_{il}$). The $x_l\sqrt{\rho^{\text{TX}}}$, where ($\rho^{\text{TX}}$ represents the average dispersed power) represents the ($\text{N} \times 1$) symbols vectors that are transmitted simultaneously by UEs. Moreover, the $n_l$ is the Additive White Gaussian Noise (AWGN) vector. The $g_{il}$ written as $g_{il} = h_{il}\sqrt{\beta_{il}}$, $l$ ranges from $\{1, 2 \cdots N\}$, and $h_{il}$ is the flat-fading coefficient from $l^{\text{th}}$ UE and $i^{\text{th}}$ BS antenna. It symbolizes the signal fading because of obstacles such as large building and moving vehicles, and also due to the extension distance signals propagation from BS to UE, where $h_{il}$ represents channel vector given as $h_{il} \sim \text{CN}(0, (\boldsymbol{\beta}_{il}\boldsymbol{I}_{\mathbf{m}}))$. The $(h_{il})$ are the channel vector entries that define the propagation channel among the $l^{\text{th}}$ UE and $i^{\text{th}}$ BS antenna. $\beta_{il}$ is the shadow fading and attenuation coefficient and $I_M$ signifies the identity matrix. The three precoding schemes including MMSE are used to carry out the downlink tasks of uplink data detection and data precoding. The LS-MIMO transmitter reduces interuser interference by using the precoding like spatial signal processing methods. Supposedly, the BS is capable of obtaining perfect channel information by uplink pilot sequences. Therefore, the results of ZF are gotten for single-cell scenario and also (with perfect CSI) for MMSE and MRT/C. The $Q = [q_1, q_2, \cdots, q_i] \in \mathbb{C}^{M \times N}$ represents the uplink linear received matrix in which the $q_i$ the column is assigned to the $i^{\text{th}}$ UE. As the ZF, MMSE, and MRT/MRC schemes are employed, therefore, the precoding matrix classification in uplink can be taken as in (3) [20]:

$$Q = \begin{cases} H\left(H^H H\right)^{-1} & \text{ZF} \\ H\left(H^H H P^{UL} + \sigma^2 I\right)^{-1} & \text{MMSE} \\ H & \text{MRT.} \end{cases} \tag{3}$$

In (3), $(.)^H$ and $(.)^{-1}$ represent the Hermiston matrix and inverse transpose, individually. Further, $H = [v_{i,1}, v_{i,2}, \cdots, v_{i,N}] \in \mathbb{C}^{M \times K}$ includes the channel values for all the UEs, and the power vector for uplink is $P^{ul} = \text{diag}\,[p_1^{UL}, p_2^{UL}, \cdots, p_i^{UL}] \in \mathbb{C}^{\text{N} \times \text{N}}$. The ZF precoding is capable of attaining the efficiency and the capacity of the network, if receiver has exemplary channel information (CSI) for a large number of UEs. Contrarily, the defective CSI at the BS the completion of ZF declines sustainably to the precision of the channel information [24]. To get the full

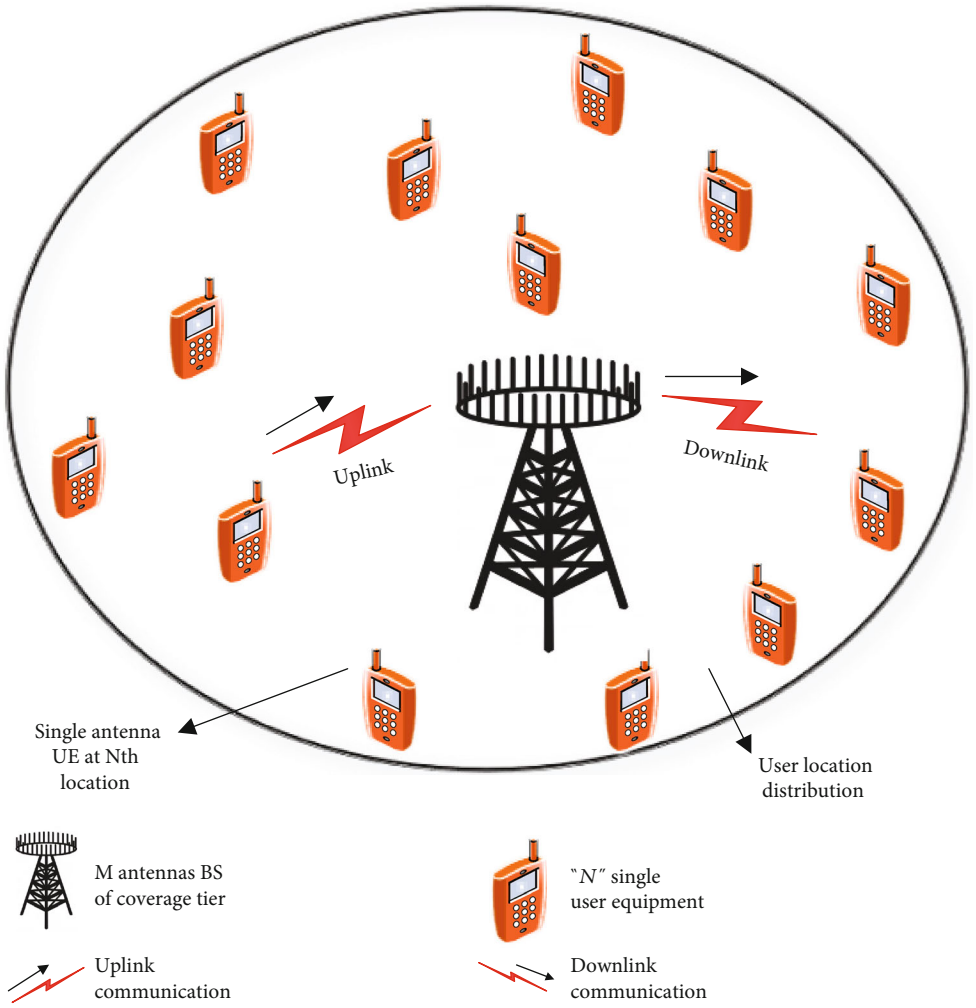


Figure 2: Uplink/downlink UE distributions in single-cell scenario: $M$ antenna BS and $N$ solo antenna UEs.

multiplexing gain, ZF demands immense overhead addressing the signal-to-noise ratio (SNR). Defective CSI outcomes as of the turn-out loss due to interuser interference. The interference continues until the users are unable to form an independent beam for independent communication. For downlink communication, linear processing schemes are characterized as $V = [v_1, v_2, \cdots, v_N] \in \mathbb{C}^{M\times N}$. The $V$ matrix is modeled as in (4):

$$\mathrm{V} = \begin{cases} H\left(H^H H\right)^{-1} & \text{ZF} \\ H\left(H^H H\, P^{UL} + \sigma^2 I\right)^{-1} & \text{MMSE} \\ H & \text{MRC.} \end{cases} \tag{4}$$

According to the equation [19], $Q = V$ to reduce the calculus complexity. The MRC is basically a diversity combining precoding scheme that combines the signals from each channel and then adds them, and alternatively, it is known as a predetection combining scheme [27]. For independent AWGN, it is used as a combiner and also reinstates a signal to its original form. The $N^{\text{th}}$ user terminal (UE/UTs) is actually located on $x_N$ $(x_N \in \mathbb{R}^2)$ measured in meters.

All users are randomly distributed in the cell. The $x_N$ is calculated w.r.t BS with the Round Robin (RR) selection; UEs are wisely selected for the communication, and the UE locations are reserved with arbitrary variables from the user distribution as shown in Figure 2. The distances from BS to UEs are comparatively greater than the range among BS antennas of the array configuration. Suppose that $(r)$ denotes the max distance of a UE and $(d_m)$ represents the min distance a UE has from BS. All UEs are spread around the BS evenly. Further, UE's location is designated by $f(x)$ modeled as (5) [19].

$$f(x) = \begin{cases} \left(\pi\left(r^2 - d_m^2\right)\right)^{-1} & d_m \le \|x\| \le r \\ 0 & \text{otherwise.} \end{cases} \tag{5}$$

Additionally, $\zeta$ represents the large-scale fading given as $\zeta = (\omega/\|x\|^{\varphi})$. $\varphi$ is $(\varphi > 2)$ path loss exponent and constant $\omega > 0$ symbolizes the attenuation factor in the channel at $d_m$. Lastly, in modeling, the invers–channel attenuation can be calculated as follows [19]:

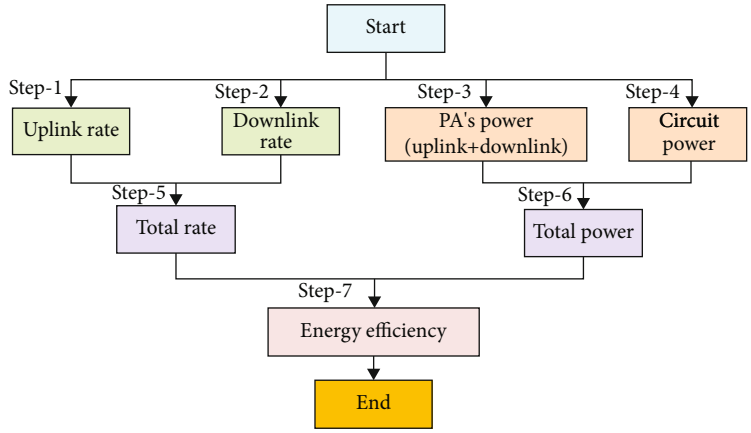


Figure 3: Computational flow.

$$E = \mathbb{E}\left((\zeta)^{-1}\right) = \left\{ \frac{\left(r^{\varphi+2} - d_m^{\varphi+2}\right)}{\left((1+(\varphi/2))\left(r^2 - d_m^2\right)\omega\right)} \right\}. \quad (6)$$

## 3. Methodology and Calculations

By applying MMSE, ZF, and MRT/C precoders, the improvement in EE of a massive MIMO system and the modeling of the optimized power consumption are the prominent objectives of this work. We have explored the methodology of energy consumption in which energy is saved by installing low-power BS according to the traffic requirements. This is a distinguished approach to reduce the consumption of power, by cutting the infrastructure cost and managing the spectrum efficiently [20]. The power consumed at the BS depends upon the total number of dynamics transmit antennas against the number of UEs obliged simultaneously.

Calculations performed in this section are shown in Figure 3. The uplink and downlink communication data rates are calculated in the first and second steps. Moreover, the right side of the flow diagram displays computations of power consumption by power amplifiers and circuitry at the BS and UEs. Further, the data rate totaled as an average. The rate in the step of total rate and the power consumption calculations are added to find the total power expended.

Lastly, the seventh step delivers the ration of average data rate and the overall power dissipation used to compute EE. Subsequent portion provides the detailed computations given in Figure 3.

*3.1. Average Data Rate.* The upper left portion of Figure 3 contains two steps for the computation of the average rate. Conferring to (7), the average rate is a summation of achievable data rate downlink and in uplink communications. We aimed to calculate the total achievable data rate for $i^{\text{th}}$ UE is given as

$$R_i^{\text{tot}} = R_i^{\text{UL}} + R_i^{\text{DL}}, \quad (7)$$

where $R_i^{\text{UL}}$ is achievable data rate in uplink and $R_i^{\text{DL}}$ represents the downlink data rate. By the Gaussian codebooks, the uplink achievable data rate is given as (8) [3]:

$$R_i^{\text{UL}} = \bar{R}_{\text{UL}}\left(\gamma^{\text{UL}}\left(1 - \frac{L^{\text{UL}}N}{S_{\text{CB}}\,\gamma^{\text{UL}}}\right)\right), \quad (8)$$

where $\gamma^{\text{UL}}$ is the uplink transmission fraction and $L^{\text{UL}}$ represents the uplink pilot length. Moreover, $[1 - ((L^{\text{UL}}N)/(S_{\text{CB}}\,\gamma^{\text{UL}}))]$ is the pilot overhead value, and the gross rate (excluding overhead factors) is given as $[\bar{R}_{\text{UL}} = B\log(1+\Phi_1)]$, where $\Phi_1$ is calculated as (9):

$$\Phi_1 = \frac{\left(p_i^{UL}\left|q_i^H h_i\right|^2\right)}{\sum_{l=1,l\neq i}^{i} p_l^{UL}\left|q_i^H h_l\right|^2 + \sigma^2\|q_i\|^2} \quad (9)$$

where $\sigma^2$ shows the noise power and $P^{\text{UL}} = [p_1^{UL}, p_2^{UL}, .., p_i^{UL}]^T$ is the uplink power allocation. In [22], the power distribution vector in uplink is $p^{\text{UL}} = \sigma^2(Z^{\text{UL}})^{-1}1_i$, and $(I, l)$ are elements of $Z^{\text{UL}} \in \mathbb{C}^{N\times N}$ given as (10):

$$\left[Z^{\text{UL}}\right]_{N,l} = \begin{cases} \dfrac{\left(\left|q_i^H h_i\right|^2\right)}{\left(\left(2^{\bar{R}/B} - 1\right)\|q_i\|^2\right)} & \text{, for } i < l \\ -\dfrac{\left(\left|q_i^H h_i\right|^2\right)}{\|q_i\|^2} & \text{, for } i \neq l. \end{cases} \quad (10)$$

According to [21], if zero-forcing precoder is applied where $M \geq N+1$, and gross rate $= B\log(1+\rho(M-N))$, where $\rho$ is proportional to the received SINR that is a designed parameter. According to the Gaussian codebooks, the downlink rate for perfect CSI is given as in (11)L

$$R_i^{\text{DL}} = \bar{R}_{\text{DL}}\left(\gamma^{\text{DL}}\left(1 - \frac{L^{\text{DL}}N}{S_{\text{CB}}\,\gamma^{\text{DL}}}\right)\right), \quad (11)$$

where $\gamma^{\text{DL}}$ is the downlink transmission fraction and $L^{\text{DL}}$ is the downlink-pilot length; the pilot overhead can be modeled as $[1 - ((L^{\text{DL}}N)/(S_{\text{CB}}\,\gamma^{\text{DL}}))]$, and the gross rate is given as $(\bar{R}_{\text{DL}}) = [\bar{R}_{\text{DL}} = B\log(1+\Phi_2)]$. The value of $\Phi_2$ is (12):

$$\Phi_2 = \frac{p_i^{DL}\left(\left(\left|h_i^H v_i\right|^2\right)/\left(\|v_i\|^2\right)\right)}{\sum_{l=1,l\neq i}^{N} p_l^{DL}\left(\left(\left|h_i^H v_i\right|^2\right)/\left(\|v_i\|^2\right)\right)+\sigma^2}. \tag{12}$$

where $p^{\mathrm{DL}} = \sigma^2(Z^{\mathrm{DL}})^{-1}$ is the downlink power vector and $(i, l)$ is the component of $Z^{\mathrm{DL}} \in \mathbb{C}^{N\times N}$. Fraction values of $Z^{\mathrm{DL}}$ are cast off to compute the realizable rate for forward link.

$$\left[Z^{\mathrm{DL}}\right]_{N,l} = \begin{cases} \dfrac{\left(\left|h_i^H v_i\right|^2\right)}{\left(2^{R/B}-1\right)\|v_k\|^2} & \text{, for } i < l \\ -\dfrac{\left(\left|h_i^H v_i\right|^2\right)}{\left(\|v_l\|^2\right)} & \text{, for } i \neq l. \end{cases} \tag{13}$$

The results of (8) and (9) are plugged in (7) to calculate the achievable rate for $i^{\mathrm{th}}$ as (14), where $\bar{R}$ is taken as the gross rate, and it is computed by totaling up the achievable data rates for bidirectional communications.

$$R_i^{\mathrm{tot}} = \left(N - \left(\frac{N\left(L^{\mathrm{UL}} + L^{\mathrm{DL}}\right)}{S_{\mathrm{CB}}}\right)\bar{R}\right). \tag{14}$$

*3.2. Computations of Power Consumptions.* The total power consumption is the summation of power dissipated by a power amplifier (PA) and also consumed by circuit components (of UEs and BS) [24], as our goal is the proposition of a power distribution model to elevate the EE based upon data rates. It is stimulating because (1) of the difficulty level of associated iterative algorithms and (2) uncontrolled positioning and a massive number of BS antennas that make it difficult to define an unapproachable cluster (set of BS antennas) without focusing to the external interference [25]. Accordingly, we have executed a more reliable, more detailed, and realistic model to calculate the power consumption of the massive MIMO system that includes all aspects of energy consumption including transmit power and component power consumption at UEs and BS, modeled as (15):

$$P_{\mathrm{total}} = P_{\mathrm{PA}} + P_{\mathrm{Cir}}^{\mathrm{total}}. \tag{15}$$

In (15), $P_{\mathrm{PA}}$ is the power consumption by PA and $P_{\mathrm{Cir}}^{\mathrm{total}}$ is represented as circuit power consumption, correspondingly. In previous works, the calculations of total circuit power are considered as ($P_{\mathrm{Cir}}^{\mathrm{total}} = Ps$), where the $Ps$ is taken as a constant value of power consumption calculated for load-independent backhaul, control signaling, and the power required for cooling the system and baseband processor [4, 17]. This way of calculating circuit power is mistaken. As a system in which the value of $M$ grows consequently, the circuit power also shows proportional growth with $M$ (that is taken constant in existing literature). The existing circuit power consumption claims that achieving an infinite EE is conceivable by increasing $M$; however, it is impossible to attain infinite EE. An average power consumed by power amplifier is delineated by [19] as $P_{\mathrm{PA}} = B\gamma/\eta\sum_{N=1}^{N}\mathbb{E}\{p_N^{\mathrm{UL}}\}$. Henceforth, in accordance with the power consumption by PA during uplink, transmission is intended as in (16):

$$P_{\mathrm{PA}}^{\mathrm{UL}} = \frac{\rho K B\sigma^2\,\gamma^{\mathrm{UL}}}{\eta^{\mathrm{UL}}}\left(\frac{r^{\varphi+2} - d_m^{\varphi+2}}{\omega\left(1+(\varphi/2)\right)\left(r^2 - d_m^2\right)}\right). \tag{16}$$

Similarly, the downlink PA's power can be modeled as (17)

$$P_{\mathrm{PA}}^{\mathrm{DL}} = \frac{\rho \mathrm{NB}\sigma^2\gamma^{\mathrm{DL}}}{\eta^{\mathrm{DL}}}\left(\frac{r^{\varphi+2} - d_m^{\varphi+2}}{\omega(1+\varphi/2)\left(r^2 - d_m^2\right)}\right). \tag{17}$$

The overall power consumption by PA is calculated as $(P_{\mathrm{PA}}^{\mathrm{UL}} + P_{\mathrm{PA}}^{\mathrm{DL}})$ that is the sum of (16) and (17). The $(\eta_{\mathrm{PA}})$ represents the efficiency of PA given as $((\gamma^{\mathrm{UL}}/\eta^{\mathrm{UL}}) + (\gamma^{\mathrm{DL}}/\eta^{\mathrm{DL}}))^{-1}$.

$$P_{\mathrm{PA}}^{\mathrm{ZF}} = \left\{\frac{\left(\rho NB\sigma^2\right)}{\eta_{\mathrm{PA}}}\left(\frac{r^{\varphi+2} - d_m^{\varphi+2}}{\omega\left(1+(\varphi/2)\right)\left(r^2 - d_m^2\right)}\right)\right\}. \tag{18}$$

The $P_{\mathrm{Cir}}^{\mathrm{total}}$ is the sum of power used in analog components and by several signal processing [20]. Mathematical model of total circuit power consumption is provided (19):

$$P_{\mathrm{Cir}}^{\mathrm{total}} = P_t + P_{C/d} + P_b + P_e + P_l + P_s. \tag{19}$$

In (19), $P_t$ represents the power consumed in transceiver chains. It can be computed as a summation of power needed for the BS antenna array, UEs, and synthesizers. Additionally, the power consumption while coding/decoding $(P_{C/d})$ can be modeled as

$$P_b = \left(\sum_{i=1}^{N}\left(\mathbb{E}\left(R_i^{\mathrm{UL}} + R_i^{\mathrm{DL}}\right) * \left(P_{\mathrm{cod}} + P_{\mathrm{dec}}\right)\right)\right). \tag{20}$$

The load-dependent backhaul is represented by $P_b$ (used for data transmission between BS and core network), and it is directly proportional to the average sum data rate. Hence, it can be further modeled as the sum of average rate during uplink and downlink communications as (21), whereas $P_{bt}$ is required by backhaul traffic power (measured in Watt/bits/sec).

$$P_b = \left(\sum_{i=1}^{N}\left(\mathbb{E}\left(R_i^{\mathrm{tot}}\right) * P_{bt}\right)\right). \tag{21}$$

We have considered $(B/S_{\mathrm{CB}})$ coherence block/seconds, and the estimation of the channel is also executed once for each coherence block. BS performs channel estimation by getting $(M \times NL^{\mathrm{UL}})$ matrix from UE and multiplying it by pilot-sequence length $(NL^{\mathrm{UL}})$ [3]. Moreover, $P_e$ represents the power used in the estimation of channel state given as $[P_e = P_e^{\mathrm{UL}} + P_e^{\mathrm{DL}}]$ and further modeled in (22)

$$P_e = \left\{ 2BN^2 \left( ML^{\mathrm{UL}} + \frac{\left(2\,L^{\mathrm{UL}}\right)}{S_{\mathrm{CB}}\Psi_{\mathrm{UE}}} \right) \right\}. \tag{22}$$

Moreover, $P_l$ is used to represent the power disbursed while applying linear processing schemes at BS. Two categories of power are measured in linear processing: the first type is required while calculating $Q$ and $V$, and the other is needed for matrix-vector multiplication by each data symbol [23]. The precoding/decoding matrices are calculated once in every coherent block while its complexity is contingent on the type of scheme. Hence, for MRT/MRC, power consumption is given as (23)

$$P_l^{\mathrm{MRC/MRT}} = \left\{ \frac{2\mathrm{MNB}}{\Psi_{\mathrm{BS}}} \left( 1 - \left( \frac{L^{\mathrm{UL}} + L^{\mathrm{DL}}}{3S_{\mathrm{CB}}} \right) \right) + \left( \frac{3\mathrm{BMN}}{S_{\mathrm{CB}}\Psi_{\mathrm{BS}}} \right) \right\}. \tag{23}$$

Moreover, the power consumed for ZF is approximately modeled as (24)

$$P_l^{\mathrm{ZF}} = \left\{ \left( \frac{BN^3}{3S_{\mathrm{CB}}\Psi_{\mathrm{UE}}} \right) + \left( \frac{BM\left(3N^2 + N\right)}{\Psi_{\mathrm{BS}}} \right) \right\} \tag{24}$$

where $\Psi_{\mathrm{LS}} = 12.8$ and $\Psi_{\mathrm{UD}} = 5G\mathrm{flops}/W$ are computational efficiency symbols of UE and BS [19]. Lastly, the power consumed while using MMSE is modeled as (25):

$$P_l^{\mathrm{MMSE}} = \left\{ \left( \frac{BN^3}{3S_{\mathrm{CB}}\Psi_{\mathrm{UE}}} \right) + \left( \frac{BM\left(3N^2 + N\right)}{\Psi_{\mathrm{BS}}} \right) \right\}, \tag{25}$$

where $P_s$ is supposed as a fixed power required for baseband, cooling, and control signaling.

*3.3. Optimization of M, N, and ρ.* The optimized value of $M$ can be symbolized as ($M^{\mathrm{optim}}$) and further intended as (26):

$$M^{\mathrm{optim}} = \left\{ \left( (\rho N - 1) + e^{W\left(\rho^2 \left(\frac{1}{e}\left(\frac{(P_{PA}+\alpha_1)}{\alpha_2}\right)+(N-1)\right)+1\right)} \right)/\rho \right\}, \tag{26}$$

where the values $\alpha_1, \alpha_2 > 0$ and $P_{\mathrm{PA}}$ is specified as PA's power consumption calculated as in (18), where $\alpha_1$ and $\alpha_2$ are power consumed by components at UE and BS given as (27) and (28):

$$\alpha_1 = \frac{\left\{ \left(4\,B\left(L^{UL}/S_{CB}\Psi_{UE}\right)\right)N^2 + \left(B/3S_{CB}\Psi_{BS}\right)N^3 \right\}\left\{ \left(P_{fix} + P_{syn}\right) + \left(P_{UE}\right) \right\}}{N}, \tag{27}$$

$$\alpha_2 = \frac{\left(B\,(2 + 1/S_{CB})/\Psi_{BS}\right)N + \left(B\left(3 - 2L^{DL}\right)/S_{CB}\Psi_{BS}\right)N^2 + \left(P_{BS}\right)}{N}. \tag{28}$$

The theorem in (26) shows the selection $M$ by the prescribed system whereas (26) displays that the optimal value is independent of rate-dependent power including the power required for the backhaul traffic and the power consumed in channel coding/decoding. Conversely, it increases by increasing the rate-independent powers such as power required by synthesizers, components of UE, and fixed power for control signaling. The lower bound of optimal $M$ can be calculated as (29):

$$M^{\mathrm{optim}} \geq \left\{ \frac{\left(P_{PA}/\alpha_2\right) + \left(\alpha_1/\alpha_2\right) + N + \left(1/\rho\right)}{\ln\left(\rho\right) + \ln\left(\left(P_{PA}/\alpha_2\right) + \left(\alpha_1/\alpha_2\right) + N + \left(1/\rho\right)\right) - 1} \right\} + \left(N\right) - \left(\frac{1}{\rho}\right). \tag{29}$$

The optimized transmit power is represented by ($\rho^{\mathrm{optim}}$) and calculated by using the Lambert function in (30)

$$\rho^{\mathrm{optim}} = \frac{\left\{ e^{W(\rho(((M-N)\,(\alpha_1 + M\alpha_2)/e)(N/P_{PA})+(1/e))+1)} - (1) \right\}}{M - N}, \tag{30}$$

where $\alpha_1$ and $\alpha_2$ are given in (31) and (32), respectively.

$$\alpha_1 = \frac{\left\{ \left(4\,B\left(L^{\mathrm{UL}}/S_{\mathrm{CB}}\Psi_{\mathrm{UE}}\right)\right)N^2 + \left(B/3S_{\mathrm{CB}}\Psi_{\mathrm{BS}}\right)N^3 \right\}\left\{ \left(P_{\mathrm{fix}} + P_{\mathrm{syn}}\right) + \left(P_{\mathrm{UE}}\right) \right\}}{N}, \tag{31}$$

$$\alpha_2 = \frac{\left(B\,(2 + 1/S_{\mathrm{CB}})/\Psi_{\mathrm{BS}}\right)N + \left(B\left(3 - 2L^{\mathrm{DL}}\right)/S_{\mathrm{CB}}\Psi_{\mathrm{BS}}\right)N^2 + \left(P_{\mathrm{BS}}\right)}{N}. \tag{32}$$

The $\rho^{\mathrm{optim}}$ is also independent of the rate-dependent power defined previously, such as power consumption during coding and decoding and power required by the backhaul traffic; however, it grows with fixed power and also with the power required by UEs and BS components for site cooling and control signaling, etc. If the large circuit powers are used, in that case, the greater PA power $P_{\mathrm{Tx}}^{\mathrm{total}}$ can be afforded by the network, meanwhile $P_{\mathrm{Tx}}^{\mathrm{total}}$ has a slight influence on the overall power dissipation. The authors in [6, 10, 11] illustrate that the TDD-based system allows a power drop that can be directly proportional to ($1/M$ or $\sqrt{1/M}$ imperfect CSI), however, keeping the nonzero data rates for the value that approaches to infinity. The lower bound of $\rho^{\mathrm{optim}}$ can be intended as (33).

$$\rho^{\mathrm{optim}} \geq \left\{ \frac{\left(P_{PA}/\alpha_2\right) + \left(\alpha_1/\alpha_2\right) + N + \left(1/\rho\right)}{\ln\left(\rho\right) + \ln\left(\left(P_{PA}/\alpha_2\right) + \left(\alpha_1/\alpha_2\right) + N + \left(1/\rho\right)\right) - 1} \right\} + \left(N\right) - \left(\frac{1}{\rho}\right). \tag{33}$$

It has been intended by finding the roots of the following polynomial of (35) [16]. The calculation of optimal "$N$" for the optimal value of EE is our target. Hence, to provide critical tractability, let us suppose the summation of ("SINR$\rho N$" and in that way the power of PA) and the total numbers of BS antennas for each UE, $(M/N)$, retained as constants ($\bar{\rho} = \rho\mathrm{N}$) and ($\bar{\mu} = M/N$) with ($\bar{\rho} > 0$) and ($\bar{\mu} > 1$). Therefore, the gross rate value can be taken as $\{\bar{c} = B\log\left(1 + \bar{\rho}(\bar{\mu} - 1)\right)\}$, and the

optimal value of the number of users can be taken as

$$N^{\text{optim}} = \min_i \lfloor N_i^o \rfloor. \tag{34}$$

In (34), $\lfloor N_i^o \rfloor$ describes the positive real roots of (35).

$$\left\{ N^4 - \left( \frac{2S_{\text{CB}}}{\left(L^{\text{DL}} + L^{\text{UL}}\right)} N^3 \right) - N^2 \Lambda_2 - 2N\Lambda_1 + \left( \frac{S_{\text{CB}}\Lambda_1}{\left(L^{\text{DL}} + L^{\text{UL}}\right)} \right) \right\} = 0, \tag{35}$$

where

$$\Lambda_1 = \left( \frac{(P_s + P_t) + P_{\text{PA}}}{\left((B/3S_{\text{CB}}\Psi_{\text{BS}}) + (MB(3 - 2\tau^{\text{DL}})/S_{\text{CB}}N\Psi_{\text{BS}})\right)} \right), \tag{36}$$

$$\Lambda_2 = \frac{\left(S_{\text{CB}}/\left(L^{\text{DL}} + L^{\text{UL}}\right)\right)\left(\left(4\text{BL}^{\text{UL}}/S_{\text{CB}}\Psi_{\text{BS}}\right) + \left(B\left((2/N) + (M/NS_{\text{CB}})\right)/\Psi_{\text{BS}}\right)\right)}{(B/3S_{\text{CB}}\Psi_{\text{BS}})(MB(3 - 2\tau^{\text{DL}})/S_{\text{CB}}N\Psi_{\text{BS}})}. \tag{37}$$

As described earlier, the optimal "$N$" is the real roots of the polynomial specified in (35). Quartic polynomials have four roots, and there are basic closed-form root expressions for a polynomial [27]. Nevertheless, these closed-form expressions are overlong, that is why these are seldom used, and also, as an alternative to these expressions, many simple algorithms are used to calculate the roots with greater statistical precision [27]. The number of UEs ($N$) are affected by different parameters, to check the impact; suppose $p_l$ and $p_e$ are both nearly equal to 0. This case is mainly relevant as $p_l$ and $p_e$, basically, diminish with the computational efficiencies that are predictable to rise speedily in the future. For the prescribed case of supposing two types of power consumption equal to zero, the $N^{\text{optim}}$ will become (38):

$$N^{\text{optim}} = \left\lfloor \left( \frac{(P_s + P_t) + P_{\text{PA}}}{B/3S_{\text{CB}}\Psi_{\text{BS}} * (MB(3 - 2\tau^{\text{DL}})/NS_{\text{CB}}\Psi_{\text{BS}})} \right) \cdot \left( \sqrt{1 + \frac{S_{\text{CB}}(B/3S_{\text{CB}}\Psi_{\text{BS}} * (MB(3 - 2\tau^{\text{DL}})/NS_{\text{CB}}\Psi_{\text{BS}}))}{(L^{\text{DL}} + L^{\text{UL}})((P_s + P_t) + P_{\text{PA}})}} \right) \right\rfloor. \tag{38}$$

The equation is a decreasing function of the power needed by BS and UE circuit components that are always growing by increasing the values of $M$ and $N$. The previous subsections deliver modest closed-form expressions of $M$, $N$, and $\rho$ that enable us to get the maximization in the area throughput gains and EE. The eventual objective is to calculate joint-global optimum. As $M$ and $N$ are numerals, so the global optimum value can be found by a comprehensive exploration of overall equitable combinations of the pair $(M, N)$ and evaluate the optimal power appropriation. In extensive MIMO systems, there is a trade-off between total power consumption and achievable rate [22].

*3.4. Modeling of EE.* According to the definition of EE, it is in a bit-per-Joule [2] and computed as a ratio of avg data rate and average power dissipation. In massive MIMO networks, metric calculation of total EE holds the form of (40). It depicts a decrease in overall power used by the system that carries enhanced results, and it can be accomplished by dropping the static power consumption of the system. The EE for the prearranged system model can be evaluated by applying the proposed power consumption model. EE can be modeled as the following optimization problem.

Table 2: Simulation parameters.

| Simulation parameter | Values |
|---|---|
| Required bandwidth ($B$) | 20 MHz |
| Coherence bandwidth ($B_{\text{Coh}}$) | 180 kHz |
| Coherence time ($T_{\text{Coh}}$) | 10 msec |
| Maximum distance/cell radius ($r$) | 200 meters |
| Minimal distance ($d_m$) | 40 meters |
| Channel attenuation ($\omega$) | $10^{-3.5}$ |
| Path loss exponent ($\varphi$) | 3.76 |
| $P_{\text{s}}$, $P_{\text{C/d}}$, $P_{\text{b}}$, and $P_{\text{t}}$ | 15, 1, 3, and 0.25 Watts |
| $\sigma_c$ (reuse 1, 2, and 3) | (0.528, 0.116, 0.021) |

$$\max_{\substack{M,K\in\mathbb{Z} \\ \bar{R}\geq 0}} (\text{EE}) = \left\{ \frac{\sum_{i=1}^{M}\left(R_i^{\text{tot}}\right)}{\left(P_{Tx}^{\text{UL}} + P_{Tx}^{\text{DL}} + P_{\text{Cir}}^{\text{total}}\left(M, N, \bar{R}\right)\right)} \right\}. \tag{39}$$

An optimized value of EE single-cell scenarios is calculated by the solution of (39). We have plugged in all previously computed values, i.e., the sum rate in (14), the power consumed by the circuit components (16), and the power of power amplifiers as in (18) to outline the EE in (40).

$$\max_{\substack{M,K\in\mathbb{Z} \\ \rho\geq 0}} (\text{EE}) = \left[ \frac{\left(K - \left(K\left(L^{\text{UL}} + L^{\text{DL}}\right)/S_{\text{CB}}\right)\bar{R}\right)}{\left(\left(\left(\rho kB\sigma^2/\eta_{\text{PA}}\right)\left(\left(r^{\varphi+2} - d_m^{\varphi+2}/\omega\left(1 + (\varphi/2)\right)\left(r^2 - d_m^2\right)\right)\right)\right) + P_{\text{Cir}}^{\text{total}}\right)} \right]. \tag{40}$$

The relationship shows a trade-off between total power dissipation and data rate [21]. EE can be improved by increasing the antennas where the total power dissipates, and it also grow proportionally.

## 4. Results and Discussion

This section provides the performed simulation results and discussion on the predefined model. We have considered an appropriate number $M$ for the EE calculations with ZF, MMSE, and MRC/MRT precoding schemes. The UEs are dispersed inconstantly; thus, the large-scale fading is demonstrated using $\zeta = (\omega/\|x\|^{\varphi})$ where $\omega$ and $\varphi$ values are given in Table 2.

The efficiency of PA for BS and UEs is given as 0.4 and 0.3, respectively. The remaining parameters used for simulation purpose are listed in Table 1, consistently stirred by the previous task in [19]. We have examined an appropriate approach to model power consumption illustrated in Methodology and Calculations. After the initialization of

```
Proposed algorithm:
Step 1:  According to Table 1, initialize the simulation parameters
Step 2:  Calculate the orthogonal pilot sequences and inverse-channel attenuation
Step 3:  If
             MRT = true || MMSE = true
Step 4:  For
             M =1: N max;
             Calculate RF power; Circuit Power; SINR and opt EE
         end
Step 5:  if ZF algorithm = true
             Compute circuit power; RF power; opt EE; and SNIR
             M opt, N opt, and optimum power.
         end
Step 6:  Plot of figures
         EE for single and multicell; RF; antenna power, and area throughput.
```

Algorithm 1: Sequence of simulation.

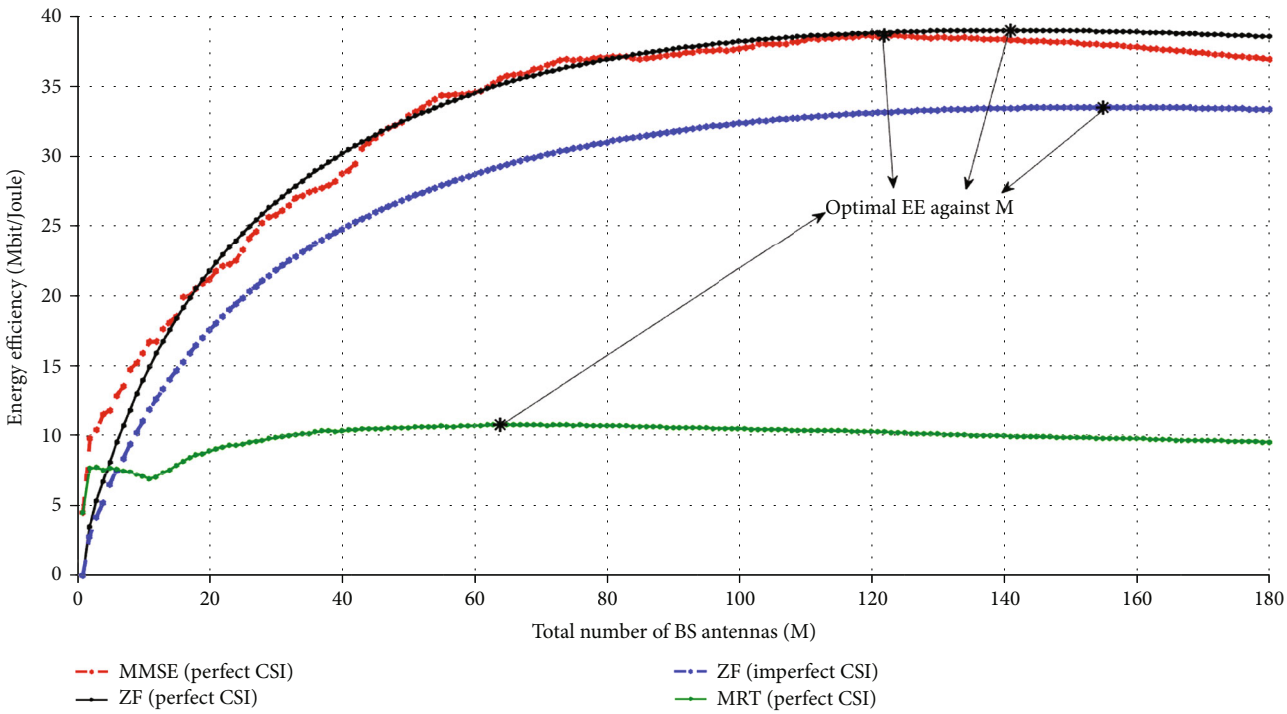


Figure 4: EE performance comparison.

simulation parameters provided in Tables 1 and 2, Algorithm 1 provides the simulation algorithm that gives computations of flow chart given in Methodology and Calculations and optimized values of the parameters to draw the figures.

*4.1. EE Performance Comparison.* In Figure 4, the results of EE vs. transmit antennas in the single-cell (MRT/C with perfect CSI, ZF with perfect and imperfect CSI, and MMSE with perfect CSI) are shown. By comparing these results with the results of previous work in [16, 19], the purposed model demonstrates improved performance.

Table 3 demonstrates the contrast of all the outcomes in which the peak value of EE contrary to the number of BS antennas in a single-cell scenario (with perfect/imperfect channel state information) gives 15% improved results with

Table 3: Comparison: results in Figure 4 and prior works.

| Linear processing scheme | Results (proposed model) | | Results [2, 13] | |
|---|---|---|---|---|
| | EE | *M* | EE | *M* |
| MMSE-perfect CSI | 38 | 122 | 30 | 165 |
| ZF-perfect CSI | 39 | 141 | 31 | 165 |
| ZF-imperfect CSI | 31 | 155 | 26 | 185 |
| MRT/C-perfect CSI | 10 | 82 | 8.0 | 85 |

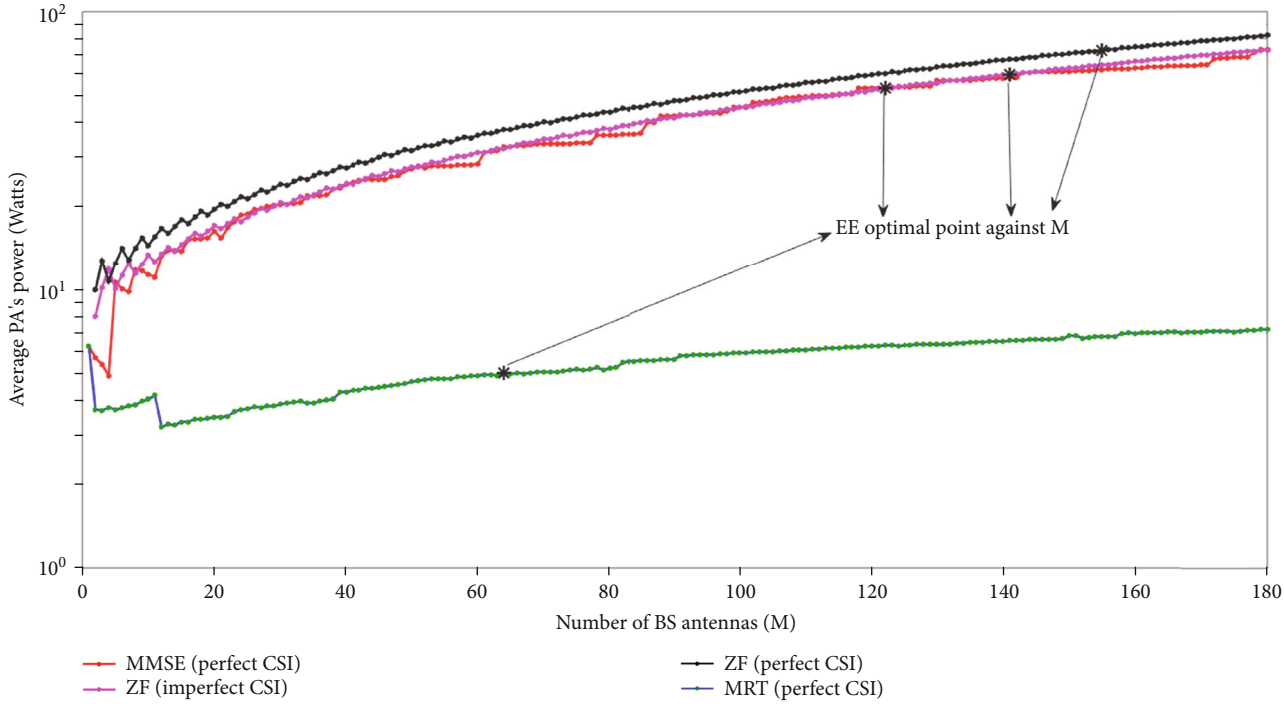


Figure 5: Comparison of PA's power consumption.

a smaller $M$. The results publicized in Figure 4 also portray that we can be able to make a more energy-efficient system by minimizing the cell size and $Ps$.

Moreover, the PA's power dissipation that exploits EE for optimal $N$ with $M$ is given in Figure 5. The MMSE has power dissipation of 50 Watt, and ZF with perfect and imperfect CSI is 55 and 70 Watts, respectively, whereas for MRT/MRC, the value is 5 Watt that is quite small as compared to the MMSE and ZF. For the ZF scheme, increasing the transmit power by the growing value of $M$ is an extra energy-efficient approach.

It is similar to Corollary 8 in [19]; however, it is dissimilar as compared with the results of [9, 10] that claim that transmission power is decreased with decreasing $M$. Further, the power consumed by an antenna at BS is inversely proportional to $M$ as shown in Figure 6. According to this figure, ZF is 100 (m-Watt/antenna) and the transmit power with MSSE where MRT/C is responsible is about 200 (m-Watt/antenna) that is lesser than calculated by [21].

*4.2. Results for Area Throughput.* Figure 7 reveals a real-time advancement in the area throughput as compared with existing literature. The maximum of the improvement is achieved in the case of MMSE and ZF with imperfect CSI.

It approves that the massive MIMO with applicable interference mitigation linear precoding schemes can achieve the outstanding area throughput and EE. In sharp contrast, the deployments of a massive number of transmit antennas while using MRT/C processing are severely restraining for both tasks either the EE or the area throughput.

Comparing the numerical values of plots in Figure 7 and the results of the previous work, the given plots demonstrate that our proposed model gives noteworthy progress in terms of area throughput. Figure 8 provides a 3D plot to show the results of an appropriate number of antennas and users equipment to realize optimal values of EE. The optimal EE is achieved at $M = 160$ that serves around $N = 100$ UE efficiently. Table 4 shows the comparison of area throughput of our work existing literature. The improvement of area throughput can be significantly observed from the generated numerical results.

## 5. Conclusions

In this paper, we have examined massive MIMO systems to get optimal EE and the area throughput gains. As a first step, we have computed the average data rates of the system for uplink and downlink communications and then suggested an essentially applicable, less complex, and an energy-efficient power consumption model. We have recognized an exceptionally optimal power allocation arrangement that can achieve considerable improvement in EE and area throughput in a single-cell scenario. The simulation results reveal noteworthy implications.

The study was fundamentally founded upon uncorrelated fading, where every user can have an exclusive channel covariance matrix. The results of MMSE and MRT/MRC are produced by the Monte Carlo simulations. Although the MMSE is the optimum for throughput gain, it is observed that ZF processing provides higher efficiency gain. It is because of the complex computations of MMSE; however,

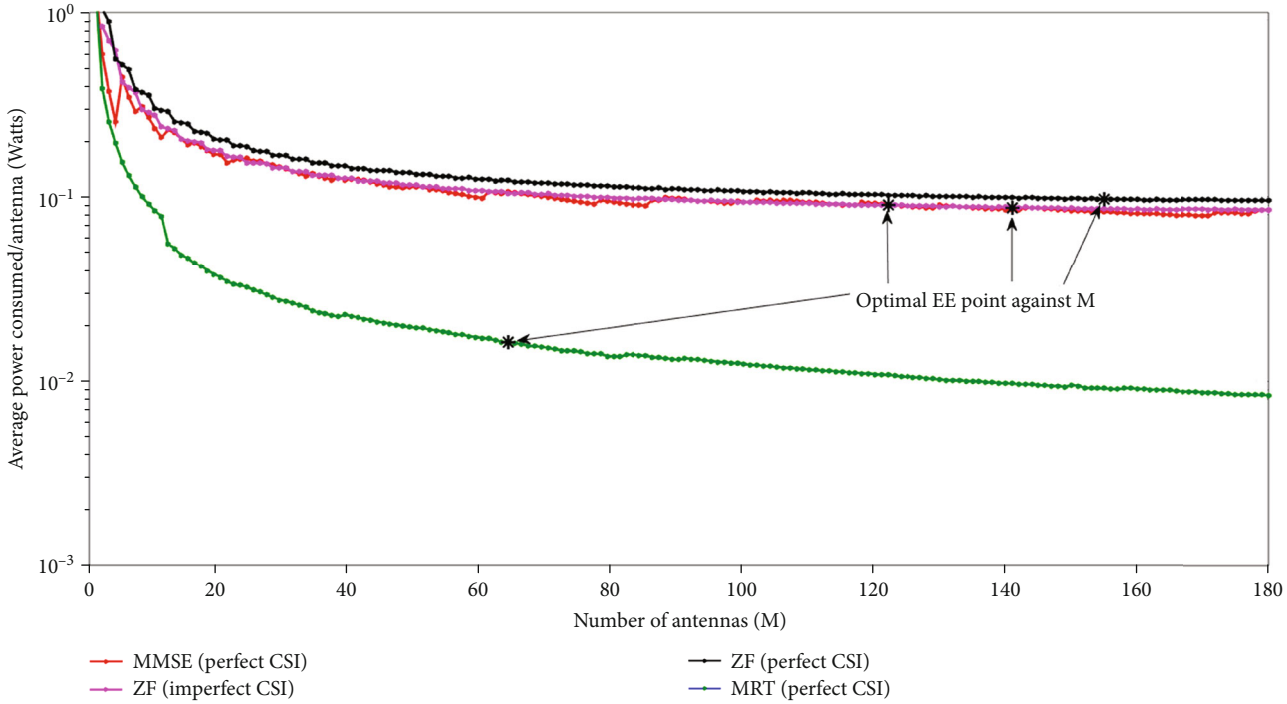


Figure 6: The power consumed by each antenna.

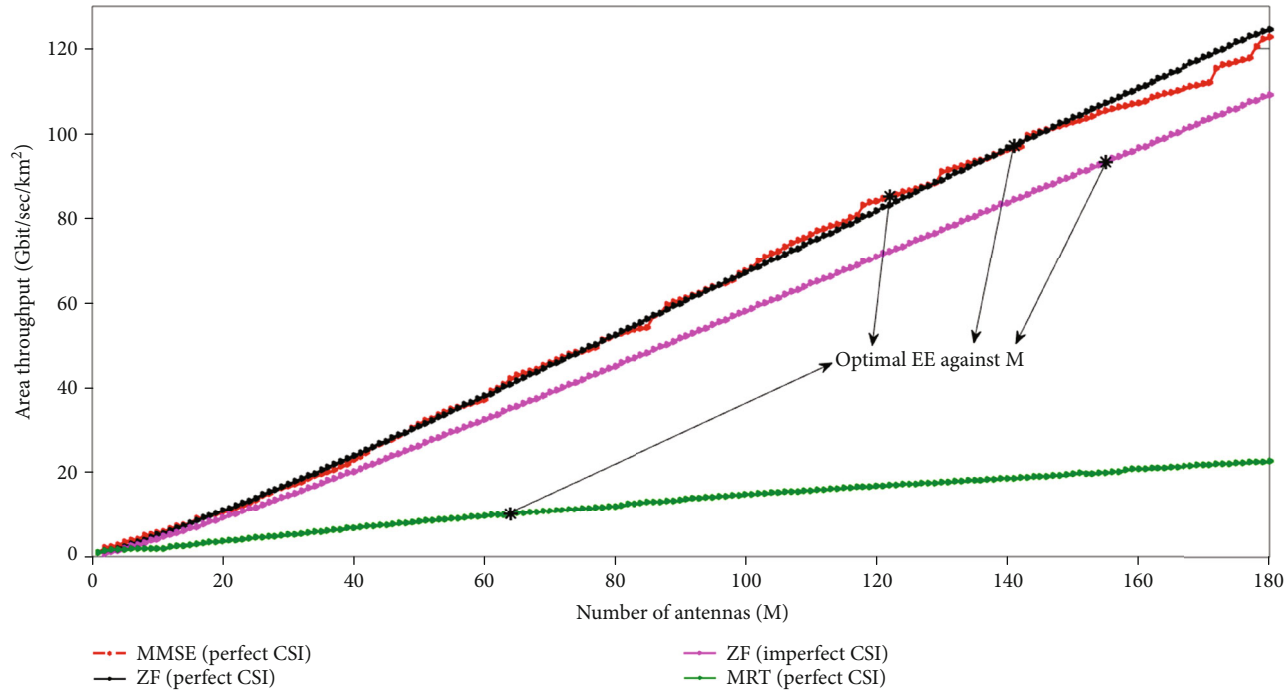


Figure 7: Area throughput in single-cell setup.

the variance in results is relatively small. The MMSE scheme has the benefit of handling the system where the value of $M < N$. The ZF precoding (with imperfect CSI) has the same performance as MMSE and ZF (with perfect CSI). The results with MRT/C are not that much good but it operates under high IUI that is why the rate/UE is less. In this scheme, complexity of signal processing is also lesser than the other schemes for the same values of $M$ and $N$; however, the power saving is not large enough to recompense the low data rates. In order to attain the same rates as ZF, the MRT/MRC needs a system where the values of $M \gg N$. Conversely, it will significantly increase the circuit power dissipation.

It is predicted that the circuit consumption will reduce with time, indicating that the higher EE can be achieved by

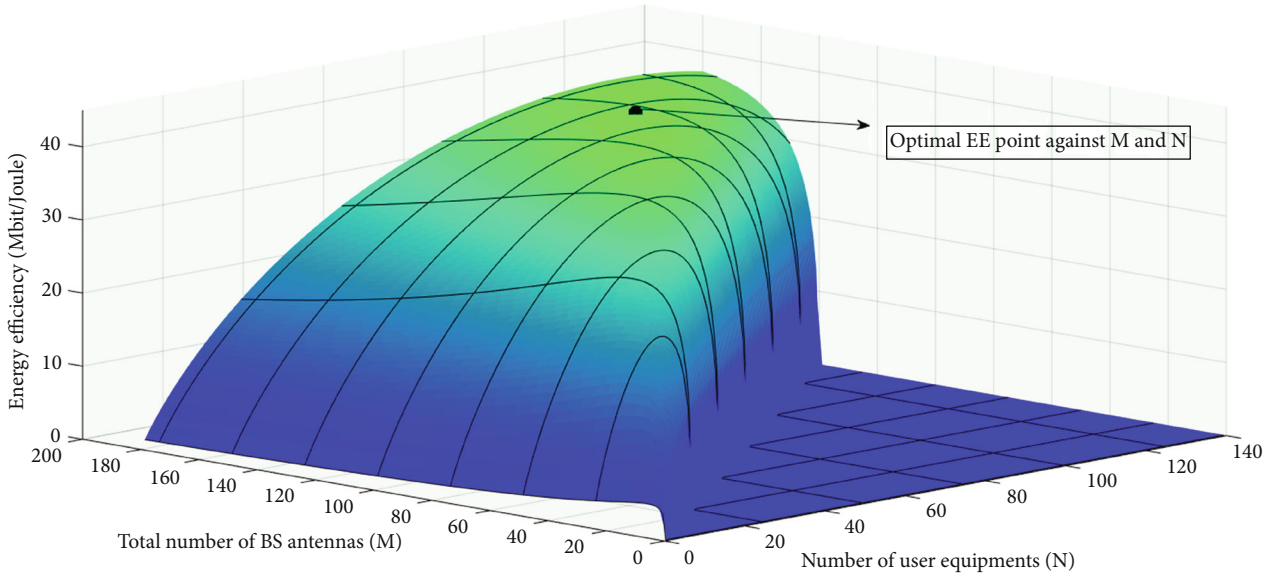


Figure 8: Appropriate number of antennas and users to realize optimal values of EE.

Table 4: Comparison of area throughput.

| Linear processing scheme | Results (proposed model) EE | Results of [2, 5] EE |
|---|---|---|
| ZF with perfect CSI | 21.0 | 15.0 |
| MMSE with perfect CSI | 82.0 | 60.0 |
| ZF with imperfect CSI | 80.0 | 62.0 |
| MRT with perfect CSI | 97.0 | 73.0 |

using fewer UEs, smaller number of BS antennas, reduced power, and progressive processing schemes. The findings of this work specify that the massive MIMO system can be built by employing a low-power transceiver (consumer grade) apparatus at coverage-tier BSs as an alternative for conservative industrial-grade high-power consuming apparatus. The decrement in power dissipation brings improved results, and it is possible by abbreviating the circuit power consumption, as the results are demonstrated in Figure 4. The ratio of reducing cell size is also applied as provided in [26] expression (40). Reducing cell radius decreases the network capacity of the system; however, it increases the EE. Conclusively, we can say the reduction in the max distance of a cell helps to expand the EE, and the reason is when we reduce the cell radius essentially, we are reducing the transmit power that results in terms of improved EE of a massive MIMO system.

## Data Availability

No data were used to support this study.

## Conflicts of Interest

The authors declare no conflict of interest.

## References

[1] J. Arshad, J. Li, and T. Younas, "Analysis and implementation of a LS-MIMO system with optimal power allocation," in *2017 IEEE 9th International Conference on Communication Software and Networks (ICCSN)*, Guangzhou, China, May 2017.

[2] J. Arshad, A. Rehman, A. U. Rehman, R. Ullah, and S. O. Hwang, "Spectral efficiency augmentation in uplink massive MIMO systems by increasing transmit power and uniform linear array gain," *Sensors*, vol. 20, no. 17, p. 4982, 2020.

[3] J. Hoydis, S. ten Brink, and M. Debbah, "Massive MIMO in the UL/DL of cellular networks: how many antennas do we need?," *IEEE Journal on Selected Areas in Communications*, vol. 31, no. 2, pp. 160–171, 2013.

[4] A. U. Rehman, R. A. Naqvi, A. Rehman, A. Paul, M. T. Sadiq, and D. A. Hussain, "A trustworthy SIoT aware mechanism as an enabler for citizen services in smart cities," *Electronics*, vol. 9, no. 6, p. 918, 2020.

[5] J. Arshad, T. Younas, L. Jiandong, and A. Suryani, "Study on MU-MIMO systems in the Perspective of energy efficiency with linear processing," in *2018 10th International Conference on Communication Software and Networks (ICCSN)*, Chengdu, China, July 2018.

[6] W. Wang, Y. Huang, L. You, J. Xiong, J. Li, and X. Gao, "Energy efficiency optimization for massive MIMO non-orthogonal unicast and multicast transmission with statistical CSI," *Electronics*, vol. 8, no. 8, p. 857, 2019.

[7] Z. Xiao, J. Zhao, T. Liu, L. Geng, F. Zhang, and J. Tong, "On the energy efficiency of massive MIMO systems with low-resolution ADCs and lattice reduction aided detectors," *Symmetry*, vol. 12, no. 3, p. 406, 2020.

[8] E. Bjornson, J. Hoydis, M. Kountouris, and M. Debbah, "Massive MIMO systems with non-ideal hardware: energy efficiency, estimation, and capacity limits," *IEEE Transactions on Information Theory*, vol. 60, no. 11, pp. 7112–7139, 2014.

[9] T. Younas, J. Li, J. Arshad, M. M. Tulu, and H. M. Munir, "New framework for analysis of EE in massive MIMO with hardware impairments," in *2018 28th International*

*Telecommunication Networks and Applications Conference (ITNAC)*, Sydney, NSW, Australia, November 2018.

[10] F. Rusek, D. Persson, Buon Kiong Lau, E. G. Larsson, T. L. Marzetta, and F. Tufvesson, "Scaling up MIMO: opportunities and challenges with very large arrays," *IEEE Signal Processing Magazine*, vol. 30, no. 1, pp. 40–60, 2013.

[11] T. Van Chien, E. Bjornson, and E. G. Larsson, "Joint power allocation and user association optimization for massive MIMO systems?," *IEEE Transactions on Wireless Communications*, vol. 15, no. 9, pp. 6384–6399, 2016.

[12] H. Q. Ngo, E. G. Larsson, and T. L. Marzetta, "Energy and spectral efficiency of very large multiuser MIMO systems," *IEEE Transactions on Communications*, vol. 61, no. 4, pp. 1436–1449, 2013.

[13] G. Miao, "Energy-efficient uplink multi-user MIMO," *IEEE Transactions on Wireless Communication*, vol. 12, no. 5, pp. 2302–2313, 2013.

[14] T. Van Chien, E. Björnson, and E. G. Larsson, "Joint power allocation and load balancing optimization for energy-efficient cell-free massive MIMO networks," 2020, http://arxiv.org/abs/2002.01504.

[15] D. Ha, K. Lee, and J. Kang, "Energy efficiency analysis with circuit power consumption in massive MIMO systems," in *2013 IEEE 24th Annual International Symposium on Personal, Indoor, and Mobile Radio Communications (PIMRC)*, London, UK, September 2013.

[16] H. Yang and T. Marzetta, "Total energy efficiency of cellular large scale antenna system multiple access mobile networks," in *2013 IEEE Online Conference on Green Communications (OnlineGreenComm)*, Piscataway, NJ, USA, October 2013.

[17] H. Khammari, I. Ahmed, G. Bhatti, and M. Alajmi, "Spatio-radio resource management and hybrid beamforming for limited feedback massive MIMO systems," *Electronics*, vol. 8, no. 10, article 1061, 2019.

[18] A. U. Rehman, M. Tariq Sadiq, N. Shabbir, and G. A. Jafri, "Opportunistic Cognitive MAC (OC-MAC) protocol for dynamic spectrum access in WLAN environment," *International Journal of Computer Science Issues (IJCSI)*, vol. 10, no. 6, pp. 45–51, 2013.

[19] E. Bjornson, L. Sanguinetti, J. Hoydis, and M. Debbah, "Optimal design of energy efficient multi-user MIMO systems: is massive MIMO the answer?," *IEEE Transactions on Wireless Communications*, vol. 14, no. 6, pp. 3059–3075, 2015.

[20] M. M. A. Hossain, C. Cavdar, E. Bjornson, and R. Jantti, "Energy-efficient load-adaptive massive MIMO," in *2015 IEEE Globecom Workshops (GC Wkshps)*, San Diego, CA, USA, December 2015.

[21] J. Wannstrom, *Further Advancements for E-UTRA Physical Layer Aspects (Release 9). 3GPP TS 36.814*, 3rd Generation Partnership Project, 2013.

[22] S. U. Pillai, T. Suel, and S. Cha, "The Perron-Frobenius theorem: some of its applications," *IEEE Signal Processing Magazine*, vol. 22, no. 2, pp. 62–75, 2005.

[23] S. Boyd and L. Vandenberghe, "Numerical linear algebra background," http://www.ee.ucla.edu/ee236b/lectures/num-lin-alg.pdf.

[24] Q. Zhang, S. Jin, M. McKay, D. Morales-Jimenez, and H. Zhu, "Power allocation schemes for multicell massive MIMO systems," *IEEE Transactions on Wireless Communications*, vol. 14, no. 11, pp. 5941–5955, 2015.

[25] D. Zhang, Z. Zhou, K. Yu, and T. Sato, "Energy efficiency scheme with cellular partition zooming for massive MIMO systems," in *2015 IEEE Twelfth International Symposium on Autonomous Decentralized Systems*, Taichung, Taiwan, March 2014.

[26] A. Kazerouni, F. Javier Lopez-Martinez, and A. Goldsmith, "Increasing capacity in massive MIMO cellular networks via small cells," in *2014 IEEE Globecom Workshops (GC Wkshps)*, Austin, TX, USA, December 2014.

[27] K. N. R. Surya Vara Prasad, E. Hossain, and V. K. Bhargava, "Energy efficiency in massive MIMO-based 5G networks: opportunities and challenges," *IEEE Wireless Communications*, vol. 24, no. 3, pp. 86–94, 2017.